© 2018. Published by The Company of Biologists Ltd | Development (2018) 145, dev147769. doi:10.1242/dev.147769

RESEARCH ARTICLE

RARγ is required for mesodermal gene expression prior to gastrulation in *Xenopus*

Amanda Janesick[1,*], Weiyi Tang[1,‡], Toshi Shioda[2] and Bruce Blumberg[1,3,§]

ABSTRACT

The developing vertebrate embryo is exquisitely sensitive to retinoic acid (RA) concentration, particularly during anteroposterior patterning. In contrast to Nodal and Wnt signaling, RA was not previously considered to be an instructive signal in mesoderm formation during gastrulation. Here, we show in *Xenopus* that RARγ is indispensable for the expression of early mesoderm markers and is, therefore, an obligatory factor in mesodermal competence and/or maintenance. We identified several novel targets upregulated by RA receptor signaling in the early gastrula that are expressed in the circumblastoporal ring and linked to mesodermal development. Despite overlapping expression patterns of the genes encoding the RA-synthesizing enzyme Aldh1a2 and the RA-degrading enzyme Cyp26a1, RARγ1 functions as a transcriptional activator in early mesoderm development, suggesting that RA ligand is available to the embryo earlier than previously appreciated. RARγ1 is required for cellular adhesion, as revealed by spontaneous dissociation and depletion of *ncam1* mRNA in animal caps harvested from RARγ1 knockdown embryos. RARγ1 knockdown obliterates somite boundaries, and causes loss of Myod protein in the presomitic mesoderm, but ectopic, persistent expression of Myod protein in the trunk. Thus, RARγ1 is required for stabilizing the mesodermal fate, myogenic commitment, somite boundary formation, and terminal skeletal muscle differentiation.

KEY WORDS: Adhesion, Mesoderm, RARγ, Retinoic acid signaling, Somitogenesis, *Xenopus*

INTRODUCTION

Retinoic acid (RA) is a signaling molecule present at discrete concentrations in precise locations throughout the developing embryo, activating gene expression where RA receptors (RARs) are expressed. The RARs are a family of three genes that encode receptor subtypes RARα, β and γ, which are ligand-modulated transcription factors in the nuclear hormone receptor superfamily (reviewed by Maden, 2007; Evans and Mangelsdorf, 2014). Where RA is absent, RARs can also function as unliganded repressors (Janesick et al., 2014). RARs possess a range of activities and developmental functions that depend on the local concentration of RA, the spatial distribution of each RAR subtype (α, β or γ) and the availability of co-activator and co-repressor proteins (Rochette-Egly and Germain, 2009).

RAR signaling is implicated in numerous developmental processes, including patterning and boundary-setting, proliferation/differentiation and organogenesis (Niederreither et al., 2001; Maden, 2007; Rhinn and Dolle, 2012; Janesick et al., 2013; Cunningham and Duester, 2015). RA is essential for the development of many non-axial mesodermal derivatives, in particular the heart, somites and kidney (Niederreither et al., 2001; Moreno and Kintner, 2004; Naylor et al., 2016). We previously showed that liganded RARβ2 in the trunk is required for somite patterning and number, hypaxial muscle migration, and restriction of the presomitic mesoderm, whereas unliganded RARγ maintains the size of the presomitic mesoderm and the pool of bipotential caudal progenitor cells (Janesick et al., 2014, 2017).

Early studies revealed that RA is unable to instruct naive ectoderm to become mesoderm. Animal caps (ectodermal explants) fail to elongate in the presence of RA (Ruiz i Altaba and Jessell, 1991; Sive and Cheng, 1991); therefore, RA signaling was not considered to have an instructive role in mesoderm formation. Furthermore, the RA-synthesizing enzyme Aldh1a2 and RA receptors are not vegetally enriched (De Domenico et al., 2015) where mesoderm inducers are located; therefore, these are unlikely to be endogenous mesoderm-inducing factors. Instead, it has been shown that RA influences mesoderm patterning after gastrulation, acting to suppress anterior and dorsal characteristics (Ruiz i Altaba and Jessell, 1991; Sive and Cheng, 1991). Nevertheless, the expression of RARγ in the circumblastoporal region of the early gastrula embryo (Pfeffer and De Robertis, 1994) led us to ask whether RA signaling is functioning earlier than initially thought.

The importance and existence of competence or maintenance factors located in the responding marginal zone has become increasingly recognized (Fletcher and Harland, 2008). It is conceivable that RARγ signaling could be such a factor, given its expression in the marginal zone, although this has not previously been addressed. Here, we provide evidence supporting a novel role for RARγ signaling in mesoderm formation. We show that the function of RARγ in mesoderm patterning after gastrulation is preceded by an earlier phase in which RARγ modulates the expression of *wnt8*, *brachyury* (*tbxt*; also known as *T*), *gdf3* and *fgf8* in the gastrula-stage embryo. Using RNA-seq, we identify several novel genes expressed in the circumblastoporal region that are upregulated by RAR signaling. We show that RARγ signaling is required for the maintenance of Myod protein in the presomitic mesoderm (PSM) domain and also find that RARγ knockdown stabilizes the muscle progenitor state, producing ectopic Myod^{+} cells in the trunk and impeding somite maturation.

[1]Department of Developmental and Cell Biology, 2011 Biological Sciences 3, University of California, Irvine, 92697-2300, USA. [2]Center for Cancer Research, Massachusetts General Hospital, Building 149, 13th Street, Charlestown, MA 02129, USA. [3]Department of Pharmaceutical Sciences, University of California, Irvine, CA 92697-2300, USA.
*Present address: Department of Otolaryngology–Head & Neck Surgery, Stanford University School of Medicine, Stanford, CA 94305, USA. ‡Present address: Division of Biology, California Institute of Technology, Pasadena, CA 91125, USA.

§Author for correspondence (blumberg@uci.edu)

A.J., 0000-0001-7731-2756; B.B., 0000-0002-8016-8414

Received 21 August 2017; Accepted 31 July 2018

Development (2018) 145, dev147769. doi:10.1242/dev.147769

RESULTS

RARγ1 is required much earlier in development than previously characterized

In 2002, Carrasco and colleagues first demonstrated that loss of retinoic acid receptor gamma 1 (RARγ1) abolished *brachyury* (*T*) and *foxa4 (pintallavis*) expression on the injected side (Fig. S1; Franco, 2002). Hence, we hypothesized that the presence of RARγ is required for the mesodermal competence or maintenance. RARγ is expressed in the circumblastoporal domain during gastrula stages, as are the genes encoding both the RA-synthesizing enzyme *Aldh1a2* and the degradation enzyme *Cyp26a1* (Fig. S2). Therefore, components of RA signaling are found in the correct time and place to regulate mesoderm development. We designed a second morpholino (MO) to *Xenopus laevis* RARγ1 in addition to the original MO used in Fig. S1, and validated specificity of the phenotype on *T* expression (Fig. S3). Loss of RARγ1 does not completely derail gastrulation (except at high MO doses), but strongly downregulates expression of genes *wnt8, gdf3* and *fgf8* in signaling pathways (Wnt, Nodal, Fgf) that are crucial for regulating mesoderm formation (Fig. 1A-D). This effect is selective for the RARγ subtype, as RARα MOs do not affect these markers (Fig. 1E-G), and *rarb* is not detectable at gastrula stages (Janesick et al., 2017). To be certain that the RARα morpholino was functional, we verified in the same clutch of embryos that RARα knockdown strongly inhibited expression of *N-tubulin* (*tubb2b*) at stage 14 (Fig. 1H) as we previously showed (Janesick et al., 2013).

Novel RA-responsive mesodermal genes are identified by RNA-seq in *Xenopus laevis*

We conducted transcriptomal analysis (Fig. S4) of gastrula-stage embryos that had been treated at early blastula (stage 6/7) with the RAR-selective agonist TTNPB, the RAR-selective antagonist AGN193109, or 0.1% ethanol vehicle control. We identified 135 differentially regulated genes (after reducing .L or .S homeolog pairs to one gene symbol) upregulated by TTNPB compared with control (Benjamini–Hochberg false discovery rate $q<0.05$, $FPKM_{VEH}>0.1$, fold change>1.5) (Table S1). We identified four genes significantly downregulated by TTNPB [*orthodenticle homeobox 2* and *5* (also known as *cone-rod homeobox*), *ADAM metallopeptidase with thrombospondin type 1 motif 1* and *betacellulin*], and no genes significantly regulated by AGN193109. If we employ a less-stringent *P*-value, the number of differentially expressed genes is substantially increased. However, we aimed for 100% validation by *in situ* hybridization, and therefore selected the more stringent q-value cut-off in these studies.

We used gene ontology (GO) analysis to assess the types of genes regulated by TTNPB in gastrula embryos and identified terms highly enriched for genes involved in known developmental roles of RA, such as regulation of homeobox proteins, embryonic morphogenesis, regionalization and patterning (Fig. 2A). Antennapedia-type homeobox genes are not typically expressed in control embryos at gastrulation, but were turned on prematurely by TTNPB (Fig. 2A). A number of Wnt signaling genes are upregulated by TTNPB, including some that promote signaling (*wnt5b*, *frizzled class receptor 4* and *10*) as well as some that antagonize signaling [*dishevelled-binding antagonist of beta-catenin 1* (*dact1*), *kringle containing transmembrane protein 2* (*kremen2*) and *zinc finger protein 703* (*znf703*)]. GO terms for neural crest, ear and hindbrain development are also highly enriched (Fig. 2A).

We selected genes for further study based on three criteria: (1) novelty (RA targets not previously characterized), (2) potential role in mesoderm development (e.g. connection to Nodal, Wnt, Fgf or Bmp pathways), or (3) regulation of mesodermal derivatives at later stages. Fig. 2B shows the FPKM values for selected genes, and we note that the expression of the .L and .S homeologs is relatively concordant. We validated the RNA-seq data by whole-mount *in situ* hybridization (WISH) (Fig. 3). Although WISH is not quantitative, we observed a positive correspondence between FPKM values and WISH signal intensity, with the exception of *MAM domain containing 2* (*mamdc2*), which we detected despite low FPKM (Fig. 3D). Probes not detected at stage 10.5 [*kielin/chordin-like protein* (*kcp*), *hyaluronan and proteoglycan link protein 3* (*hapln3*) and *follistatin like 1* (*fstl1*)] were validated at neurula or tailbud stages to show correct, published expression when this information was available on Xenbase (Karpinka et al., 2015).

znf703, *znf503*, *kremen2* and *mamdc2* are expressed in the circumblastoporal ring, but absent from the organizer (Fig. 3A-D), reminiscent of the expression patterns of *ventx2* or *wnt8* (Karpinka et al., 2015). TTNPB intensifies and expands expression of *znf703*, *znf503*, *kremen2* and *mamdc2* into the dorsal domain (Fig. 3E-H). This result is concordant with zebrafish data showing that RA causes the ortholog *Znf703* to be ectopically expressed in the embryonic shield (Andreazzoli et al., 2001). *skida1*, which normally is barely detectable, is intensified in TTNPB-treated embryos, although its domain is unchanged (Fig. 3I,M). *Nkx6-2* is found in the dorsal lip, and TTNPB widens and ventralizes its expression (Fig. 3J,N).

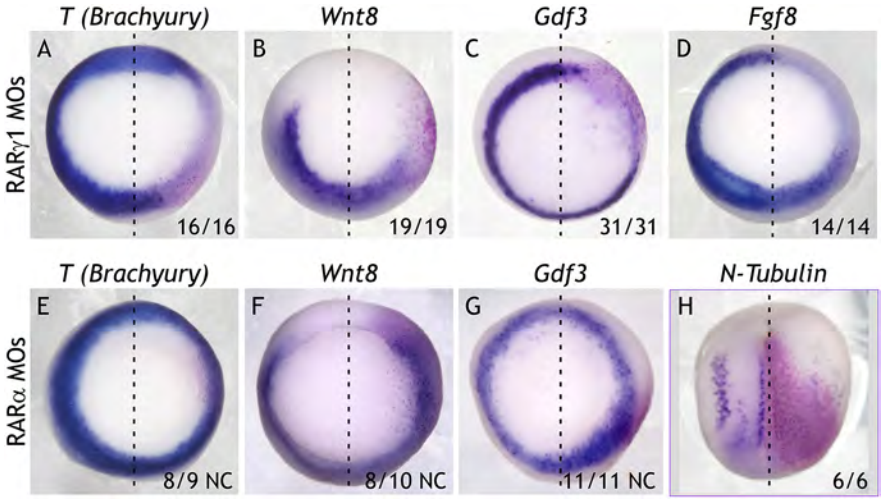

Fig. 1. RARγ1 is required for the expression of mesoderm markers. (A-D) Embryos were microinjected unilaterally at the 2-cell or 4-cell stage with 3.3 ng RARγ1.S+3.3 ng RARγ1.L/S MOs (Fig. S3). Injected side is to the right of the dashed line, and is indicated by the magenta *β-gal* lineage tracer. WISH shows that RARγ1 MOs result in the loss of *T*, *fgf8*, *wnt8* and *gdf3*. (E-H) Embryos were microinjected unilaterally at the 2-cell or 4-cell stage with 6.6 ng RARα2 MOs (Janesick et al., 2013). Injected side is to the right of the dashed line, and is indicated by the magenta β-gal lineage tracer. RARα2 MOs did not affect *T*, *wnt8* or *gdf3* expression, but did produce loss of *N-tubulin* as previously published (Janesick et al., 2013). All embryos, except in H, are shown in vegetal view at stage 10.5/11. H is shown in dorsal view, with anterior on the bottom at stage 14. Fractions represent the portion of embryos displaying the phenotype. NC, no change.

Development (2018) 145, dev147769. doi:10.1242/dev.147769

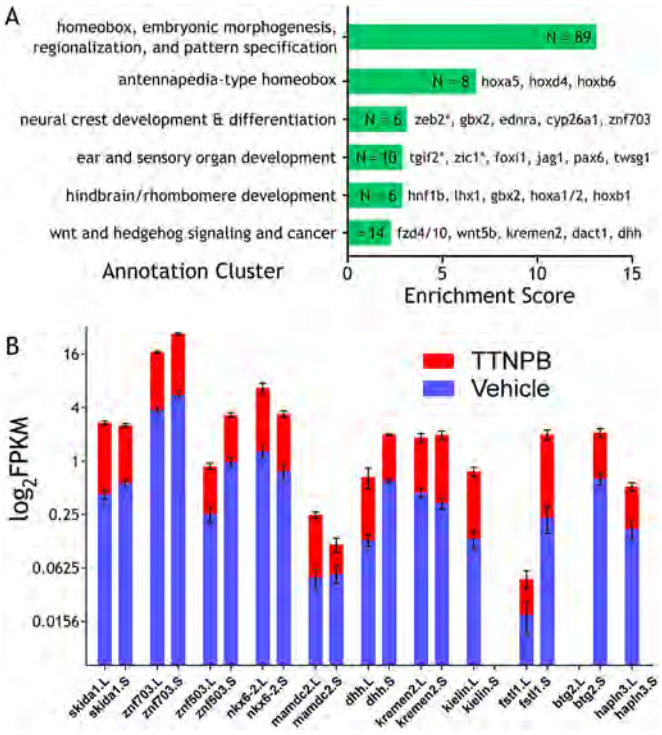

Fig. 2. Results of RNA-seq data analysis. (A) GO analysis of differentially expressed genes after TTNPB treatment. GO terms shown to be statistically over-represented (P=0.001) in 1 µM TTNPB-treated embryos (q<0.05, $FPKM_{VEH}$>0.1) conducted in DAVID (Huang da et al., 2009a, b). Gene symbols from *Xenopus* were used as input, and GO terms were derived from human (for better annotation). Enrichment score is measured by Fisher's exact statistics by the DAVID server. **zic1* is a downregulated gene, and *zeb2*, *tgif2* are <1.5-fold activated by TTNPB. (B) TTNPB-induced genes selected for further analysis in mesoderm development. Activation by TTNPB (represented as log_2FPKM) is mapped for both .L and .S subgenomes (Matsuda et al., 2015; Session et al., 2016). *kielin* and *btg2* are not found in .S and .L, respectively; *hapln.S* is not detected by RNA-seq.

dhh was not previously characterized at gastrula stages; we show that it is expressed in a punctate pattern surrounding the blastopore, and is greatly expanded by TTNPB (Fig. 3K,O). *cyp26a1* is a known direct RAR target and serves as a positive control for the effects of modulating RA signaling. *cyp26a1* expression is expanded into the animal domain accompanied by punctate, apparently nuclear staining in the vegetal tissue (Fig. 3L,P).

RARγ1 functions as an activator during mesoderm development

Considering the overlapping expression of the genes encoding the RA-synthesizing enzyme *Aldh1a2* and the RA-degrading enzyme *cyp26a1* with *rarg* mRNA expression (Fig. S2), we tested whether RARγ1 was functioning as an activator or repressor in modulating the expression of one of its targets, *znf703*. RARs are capable of both direct activation or repression of target genes depending on their proximity to ligand during development (Janesick et al., 2014). We possess expression constructs for wild-type RARγ1 (WT RARγ1), constitutively active RARγ1 (VP16-RARγ1, which mimics the liganded, active form of the receptor), and dominant-negative RARγ1 (DN-RARγ1, which mimics the unliganded, repressive form of the receptor), which were made in a similar manner to the RARα constructs previously described by Blumberg et al. (1997). Microinjection of these constructs alone led to expansion of *znf703* in VP16-RARγ1-injected embryos (Fig. S5A,B) and knockdown of *znf703* by DN-RARγ1 (Fig. S5C,D). WT RARγ1 rescues *znf703* expression as expected (Fig. 4C,G), and further confirms the specificity of our morpholino. VP16-RARγ1 rescues *znf703*, and expands its domain dorsally and animally (Fig. 4B,F; Fig. S5E) whereas DN-RARγ1 does not rescue *znf703* expression (Fig. 4D,H). Therefore, we infer that RARγ1 is functioning as a transcriptional activator during mesoderm development, and that retinoids are likely available to the embryo at this stage, earlier than previously recognized.

Explants from RARγ1 MO-injected embryos spontaneously dissociate

Xenopus animal caps can be induced to become dorsal mesoderm at high concentrations of activin (Sokol et al., 1990; Ruiz i Altaba and Jessell, 1991). We isolated animal caps from RARγ1 MO-injected embryos using a low-dose MO that does not elicit non-specific effects on gastrulation. We treated the caps with activin and found that, instead of elongating, they dissociated within 12 h irrespective of the activin concentration, compared with control MO (Fig. 5A,B). *ncam1* expression was upregulated by activin in control embryos as previously published (Bolce et al., 1992), but was significantly decreased in RARγ1 MO-injected caps at 8-h post-activin treatment (Fig. 5C), with little change in expression of the housekeeping gene *histone H4* (*hist1h4d*). This indicates that RARγ1 is required for cellular adhesion and the ability of explants to elongate. Furthermore, adhesion is also crucial for intercellular signaling required for mesodermal competence (Gurdon, 1988; Kato and Gurdon, 1993), as well as in boundary formation, where RAR is known to play a major role (e.g. in somite and rhombomere border delineation).

RARγ1 knockdown terminates the myogenesis program

One of the earliest derivatives of mesodermal induction is muscle (Gurdon et al., 1993). Soon after gastrulation begins, *myod* expression occurs in presumptive muscle in response to mesoderm induction (Hopwood et al., 1989; Harvey, 1992). Consistent with our results in early mesoderm (Fig. 1), we found that expression of *myod* mRNA was restricted and diminished on the injected side of RARγ1 MO-embryos (Fig. 6A; also see figure S13 in Janesick et al., 2014). Generally speaking, *myod* WISH staining was mostly diffuse and reduced in intensity such that the only conclusion it is possible to make confidently is that somite boundaries have been blurred or lost. Therefore, we employed an immunohistochemical approach to detect Myod protein (Hopwood et al., 1992) in coronal sections. As expected, we observed loss of unsegmented PSM expression on the injected side (Fig. 6B), which agrees with our previous finding that RARγ is required for the maintenance of the PSM (Janesick et al., 2014).

Despite the fact that Myod is frequently used as a somite marker, its presence is insufficient to assure terminal myogenic differentiation (Hopwood et al., 1991; Kato and Gurdon, 1993). Rather, continued expression of Myod inhibits terminal differentiation of skeletal muscle. We found ectopic Myod-positive nuclei throughout the trunk of the tailbud-stage embryo (Fig. 6A). Accordingly, differentiated skeletal muscle marked by 12/101 staining was significantly reduced on the injected side (Fig. 6B). We conclude that loss of RARγ1 prevents the full myogenesis program from occurring and that this phenotype is likely to be linked to deficiencies in early mesoderm formation (see Discussion).

DISCUSSION

RARγ signaling is important in early mesoderm development

RA is not considered to be an instructive signal in mesoderm induction, in contrast to Nodal and Wnt signaling. RA inhibits

Development (2018) 145, dev147769. doi:10.1242/dev.147769

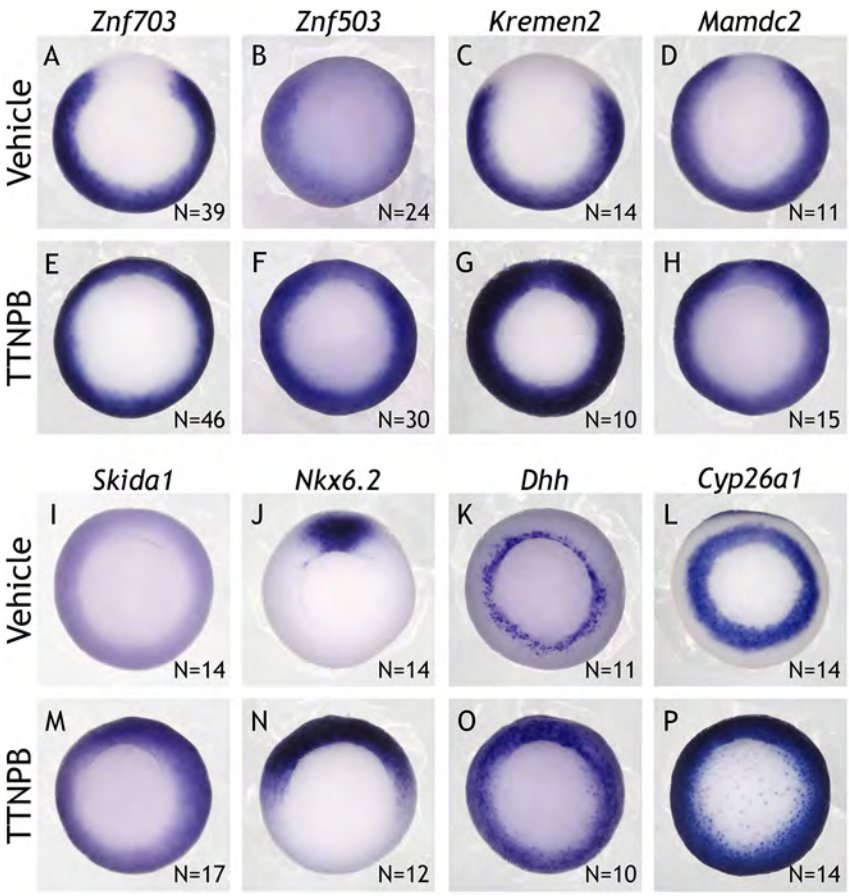

Fig. 3. RAR-selective agonist TTNPB modulates expression of genes identified by RNA-seq. (A-P) WISH from embryos treated at stage 6/7 with 1 µM TTNPB or control vehicle (0.1% ethanol). (A-D,I-L) Control expression of *znf703*, *znf503*, *kremen2*, *mamdc2*, *skida1*, *nkx6-2*, *dhh* and *cyp26a1*. (E-H,M-P) TTNPB expands expression of these genes. All embryos are shown in vegetal view at stage 10.5/11 with dorsal lip at the top. N, number of embryos scored in the experiment; 100% of embryos displayed the phenotype shown.

expression of dorsal mesoderm markers in animal caps exposed to high doses of activin, but is unable to promote elongation of caps alone (Ruiz i Altaba and Jessell, 1991; Sive and Cheng, 1991). Previous research showed that RA acts during mesoderm formation by transforming the anteroposterior value of mesoderm toward the posterior. Nevertheless, factors that serve as permissive signals or contribute to the competence of responding tissue are very important for embryonic inductions, including mesoderm induction (Fletcher and Harland, 2008). RA, in combination with BMP4, can induce the production of mesodermal precursors from embryonic stem cells (Torres et al., 2012), and many mesodermal derivatives (e.g. somites, heart, kidney, gonads) are affected when RA signaling is perturbed (Cartry et al., 2006; Hasegawa and Saga, 2012; Rhinn and Dolle, 2012, and reviewed by Cunningham and Duester, 2015; Naylor et al., 2016). Here, we propose a new role for RARγ signaling and show that it is required much earlier than had been previously thought for the expression of mesodermal markers, *in vivo*.

Retinoids are present in *Xenopus* eggs and embryos, but their availability in early development has been controversial (Pijnappel et al., 1993; Creech Kraft et al., 1994; Blumberg et al., 1996). Reporter gene studies have suggested that retinoids are not active in the embryo until neurula stages (Ang and Duester, 1999); however, 4-oxo-retinaldehyde (Blumberg et al., 1996) and 4-oxo-RA (Pijnappel et al., 1993) can activate RAR and are present in gastrula-stage embryos. Chicken embryos also possess high levels of RA in Hensen's node during gastrulation (Chen et al., 1992). Although *cyp26a1* is highly expressed in the *Xenopus*

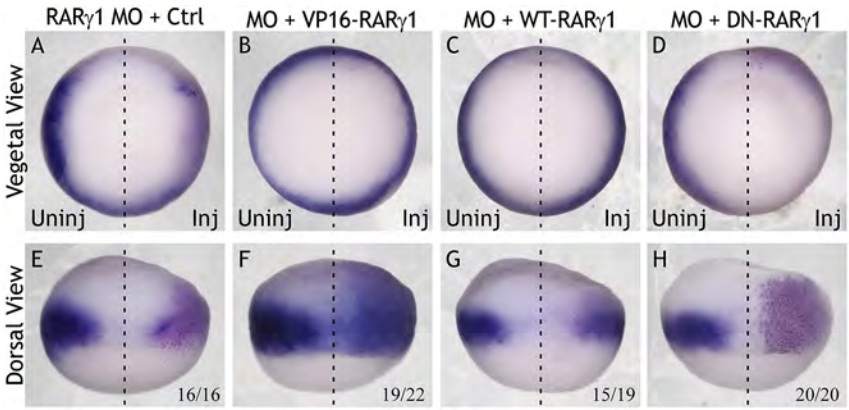

Fig. 4. RARγ1 acts as a transcriptional activator in rescuing *znf703* expression in RARγ1 MO embryos. (A-H) Embryos injected unilaterally at the 2- or 4-cell stage. Injected side is to the right of the dashed line, and is indicated by the magenta *β-gal* lineage tracer. (A,E) 3.3 ng RARγ1.S+3.3 ng RARγ1.L/S MOs diminish *znf703* expression. (B,F) VP16-RARγ1 mRNA (0.2 ng) rescues and expands *znf703* expression beyond its usual boundary. (C,D,G,H) WT RARγ1 mRNA (0.5 ng) partially rescues *znf703* (C,G) and 2 ng DN-RARγ1 mRNA does not rescue *znf703* at all, and the severity of the knockdown is increased (D,H). Embryos are shown at stage 10.5/11 in vegetal (A-D) or dorsal (E-H) view. Fractions represent the portion of embryos displaying the phenotype.

Development (2018) 145, dev147769. doi:10.1242/dev.147769

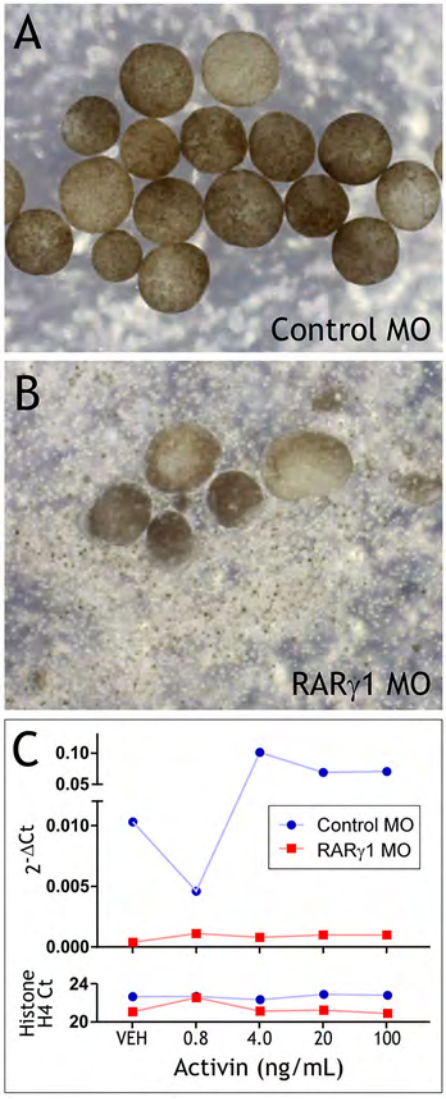

Fig. 5. RARγ1 MO inhibits cell adhesion in animal caps. (A-C) Embryos were injected bilaterally at the 2-cell stage with 3.3 ng RARγ1.S+3.3 ng RARγ1.L/S MOs. Animal caps were harvested at stage 9 and incubated in control vehicle or defined doses of activin (0.8, 4, 20 and 100 ng/ml) overnight. (A,B) RARγ1 MOs result in animal cap dissociation (note the large number of single cells) (B), compared with control MO (A) in all treatment conditions. This effect was replicated in three separate experiments. mRNA was harvested 8 h after treatment from the third and final animal cap experiment and evaluated as shown in C. (C) *ncam1* expression was significantly reduced in RARγ1 MO animal caps compared with control MO, despite constant housekeeping (*histone H4*) expression. The upper *y*-axis represents *ncam1* expression $2^{-\Delta Ct}$ values normalized to *histone H4*. The bottom *y*-axis shows raw Ct values of *histone H4*.

circumblastoporal domain, it has not been determined whether this enzymatic pathway is responsible for generating 4-oxo-retinoids, in comparison with its known activity in producing 4-OH-retinoids (Shimshoni et al., 2012; Topletz et al., 2015). We showed that only the wild-type and constitutively active forms of RARγ1 rescued mesodermal markers (e.g. *znf703*) in RARγ1-knockdown embryos. As the constitutively active form of RARγ1 mimics liganded RARγ1, our results suggest that retinoids are available to the embryo (at least locally) at gastrula stages, unless the receptor functions as an unliganded activator, which would be unprecedented for an RAR.

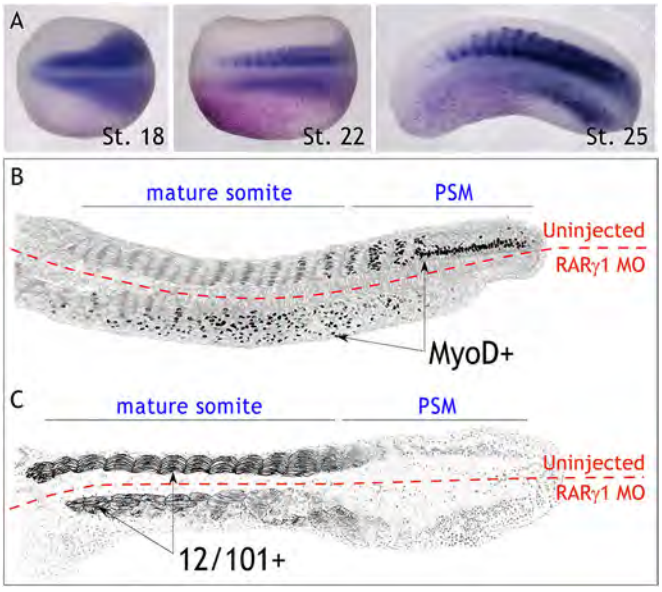

Fig. 6. RARγ1 knockdown yields a complex phenotype on *myod* mRNA and Myod protein. Embryos were injected unilaterally at 2- or 4-cell stage. (A) Injection of 3.3 ng RARγ1.S+3.3 ng RARγ1.L/S MOs lead to reduced *Myod* mRNA expression (10/14 embryos, dorsal view). (B) RARγ1 MOs cause loss of PSM expression of Myod protein and ectopic expression in the trunk of coronal sections of stage 26 embryos (4/4 embryos). (C) RARγ1 MOs cause loss and disorganization of mature somite marker 12/101 in coronal sections of stage 26 embryos (4/4 embryos).

Novel RAR targets in early mesoderm development

We identified several novel targets expressed in the circumblastoporal region that are upregulated by RAR signaling in the early gastrula. *znf703*, *znf503*, *kremen2* and *mamdc2* are normally absent from the dorsal organizer, but are ectopically expanded there in the presence of RA. Hence, RA ventralizes dorsal tissue during mesoderm development, a phenomenon already recognized in later stages, as RA-treated embryos display a *bauchstuck* (ventralized) phenotype (Durston et al., 1989; Sive et al., 1990). RA also expanded the expression domain of the ventral patterning gene *nkx6-2*. This is concordant with the observation that *Nkx6.2* is reduced in vitamin A-deficient quail as well as RAR antagonist-treated chicken embryos (Diez del Corral et al., 2003; Bayha et al., 2009).

Kremen2 is the receptor for Dickkopf, a Wnt inhibitor that mediates mesendoderm internalization and promotes head mesoderm and cardiac fate (Schneider and Mercola, 2001). *skida1*, a DACH/dachshund-related gene of unknown function, was more ubiquitously expressed than other markers, but highly responsive to RA. Its expression in the pronephric kidney at later stages (Seufert et al., 2005) could indicate a potential role of *skida1* in responding to RA signaling in pronephric precursors. *dhh* is a hedgehog gene important for mammalian Leydig cell differentiation (reviewed by Franco and Yao, 2012), and is highly expressed in *Xenopus* testis (Haselman et al., 2015). These findings could provide molecular mechanisms linking RA signaling with intermediate mesoderm and gonadal development.

Our results show that RARγ1 MO inhibits cell adhesion in animal caps which has important implications for numerous developmental processes, such as the morphogenic movements of gastrulation and the formation of somite or rhombomere boundaries. Two of the targets identified in our RNA-seq dataset regulate adhesion. Although the function of *mamdc2* is not well characterized, the MAM domain is found in proteins that regulate cell adhesion and

Development (2018) 145, dev147769. doi:10.1242/dev.147769

motility, such as zonadhesin and nephronectin (Beckmann and Bork, 1993). *znf703* is implicated in epithelial-mesenchymal transitions (EMTs), downregulates *E-cadherin* (*cdh1*), and increases cell invasion/motility (Holland et al., 2011; Slorach et al., 2011; Shahi et al., 2015). Although mesoderm formation in *Xenopus* is not considered to be a classical EMT (Nakaya and Sheng, 2008), the transformation of epithelioid cells to mobile mesenchymal cells during *Xenopus* gastrulation undoubtedly requires genes that regulate cell adhesion and morphogenesis, such as *znf703*. *znf703* is also expressed in somites and the neural plate border (Hong and Saint-Jeannet, 2017). Therefore, regulation of *znf703* by RA might be important for the epithelialization of somites as well as neural crest migration.

RARγ and mesodermal development – the bigger picture

RA can act late on myoblast, cardiac, renal or gonadal progenitor populations to affect specification or differentiation, but our results open the possibility that RARγ acts earlier to promote mesodermal fates. Loss of adhesion and subsequent dissociation in explants from RARγ1 MO-injected embryos is likely to disrupt the 'community effect' (intercellular signaling), which has been shown to be important for myogenic differentiation and the early stages of somitogenesis (Gurdon, 1988; Cossu et al., 1995). In these early studies, myogenic commitment was not solely determined by inducing signals, but additional signals (e.g. embryonic FGF ligand) within the responding tissue (Symes et al., 1988; Standley et al., 2001). One of the earliest mesodermal genes upregulated after induction is Myod, but expression of Myod alone doth not a muscle make (Hopwood et al., 1991). The fact that the injected side of RARγ1 MO tailbud embryos still expresses Myod without 12/101 indicates that cells have not received the appropriate signals (even if only from each other) to fully stabilize myogenic commitment and terminal differentiation.

In line with our previous findings (Janesick et al., 2014), injection of RARγ1 MO led to an absence of Myod protein in nuclei of the unsegmented PSM. This is expected because RARγ1 is known to play an important role in the maintenance of chordoneural hinge and unsegmented PSM (Janesick et al., 2014). However, we also observed that in RARγ1 MO-injected embryos, $Myod^{+}$ cells were found ectopically in the trunk, which could indicate that PSM identity is transformed rostrally. Alternatively, the presence of $Myod^{+}$ cells without somite maturation (as indicated by 12/101 staining) suggests that the muscle differentiation program commences, but cannot finish. In this scenario, RARγ1 loss of function might actually stabilize the muscle progenitor state, thus hindering somite maturation, or Myod might require RARγ1 for its degradation.

Unlike other manipulations of RA signaling (chemical treatment, RARβ MO injection, overexpression of constitutively active or dominant-negative RARα or RARγ), which shift somitomere boundaries or alter somitomere size (Moreno and Kintner, 2004; Janesick et al., 2014), or chevron morphology (Janesick et al., 2017), loss of RARγ is the only manipulation of RA signaling that completely precludes any somite boundaries from forming. Furthermore, genes that normally regulate boundary formation, such as *ripply2* and *thyl2* (*mespa*) are barely detectable in RARγ MO-injected embryos (Janesick et al., 2014). The RARγ MO-induced dissociation of explants is a clue that cellular adhesion, an important component of boundary formation, is perturbed. Furthermore, somite maturation requires Myod degradation for proper somite epithelialization and boundary formation. Continued ectopic Myod expression observed on the injected side of RARγ1 MO-injected tailbud embryos is likely to completely thwart a successful myogenic program.

Our finding that RARγ is required for the expression of early mesodermal markers opens the possibility that RA signaling provides a more instructive role, as opposed to simply providing positional cues to already committed tissue. Current guidance protocols for making mesoderm or muscle from stem cells in culture currently do not utilize RA (Chal et al., 2016; Loh et al., 2016). Our results suggest that RA signaling could be exploited in mesoderm formation, but with careful attention to specificity of receptor subtypes. As new receptor-selective ligands are developed (Tsang et al. 2003; Shimono et al., 2011), it will be interesting to consider whether mesodermal lineages can be further manipulated, stabilized or specialized based on the results provided here and an increased understanding of how RA receptors actually function in development.

MATERIALS AND METHODS

RNA-seq

Eggs from one clutch of female *X. laevis* were fertilized *in vitro* and embryos were staged as described (Janesick et al., 2014). Stage 6-7 embryos were treated in groups of 25 in 60-mm glass Petri dishes with 10 ml of 0.1× MBS containing 1 µM RAR-selective agonist TTNPB (Tocris), 1 µM RAR-selective inverse agonist (antagonist) AGN193109 (a gift from Dr Rosh Chandraratna, IO Therapeutics; Arima et al., 2005) or vehicle control (0.1% ethanol). Each dish was harvested at gastrula stage 10.5 in five-embryo aliquots; each aliquot was designated as n=1 biological replicate. Replicates were taken from two different clutches, and five replicates were analyzed within each clutch (ten replicates in total). Approximately ten embryos from each chemical treatment were reserved and aged until stage 40 to verify that the chemicals resulted in strong retinoid phenotypes as previously published (Koide et al., 2001).

Each five-embryo pool was homogenized in 200 µl of TriPure (Roche). Total RNA was DNAse treated, LiCl precipitated, and 100 ng was reverse transcribed into cDNA using Ovation RNA Amplification System V2 (NuGEN). Deep-sequencing libraries with barcode indices were synthesized using ABI SOLiD 5500 Fragment Library Core Kit and subjected to 50-nucleotide, single-read multiplex sequencing with ABI SOLiD 5500XL deep sequencers (Aceto, et al., 2014). The Bowtie, TopHat and Cufflinks pipeline was used (Trapnell et al., 2012), and expression data deposited in Gene Expression Omnibus under accession number GSE119124. Differential gene expression analysis (TTNPB or AGN193109 versus control) was conducted using CyberT (Kayala and Baldi, 2012) to facilitate comparison with our previously published microarray datasets (Arima et al., 2005; Janesick et al., 2014). We employed VSN normalization and performed unpaired two-conditions data analysis on FPKM (fragments per kilobase per million mapped reads) values for 1 µM TTNPB versus vehicle control, and 1 µM AGN193109 versus vehicle control. q-values from differential expression analysis are reported as Benjamini–Hochberg-corrected P-values. The full dataset of differentially expressed genes is available in Tables S1 (1 µM TTNPB) and S2 (1 µM AGN193109). We conducted GO analysis using DAVID (Database for Annotation, Visualization and Integrated Discovery; Huang da et al., 2009a, b).

Embryo microinjection and *in situ* hybridization

Xenopus eggs were fertilized *in vitro* and embryos were staged as described (Janesick et al., 2012). Embryos were microinjected bilaterally or unilaterally at the two- or four-cell stage with gene-specific MOs (Table S3) and/or mRNA together with 100 pg/embryo *β-galactosidase* (*β-gal*) mRNA lineage tracer. Both morpholinos against RARγ1 yield the same knockdown phenotype on *znf703* (Fig. S3). Embryos were maintained in 0.1× MBS until appropriate stages. Embryos processed for WISH were fixed in MEMFA (10% 10× MEMFA salt, 10% formaldehyde, 80% DEPC water), stained with magenta-GAL (Biosynth), and then stored in 100% ethanol (Janesick et al., 2012).

WISH was performed on microinjected embryos as previously described (Janesick et al., 2012). *fgf8* probe (courtesy of Nancy Papalopulu, University of Manchester, UK) was linearized with *Bam*HI. All other probes were prepared by PCR amplification of protein-coding regions (~500-800 bp) from either cDNA or library clones with a bacteriophage T7 promoter at the 3′ end. Relevant primers are listed in Table S4. Probes were transcribed with MEGAscript T7 (Life Technologies) in the presence of digoxigenin-11-UTP (Roche) as previously described (Janesick et al., 2012).

Animal cap assays

Microinjected animal caps were explanted at stage 8-9 and collected into 1% agarose, 0.4× MBS Petri dishes. Each cap was transferred to individual depressions created in a 1% agarose-coated 6-well plate, in 0.4× MBS plus activin treatment (R&D Systems recombinant Activin A) or control vehicle. After overnight incubation (~10 h), animal caps were homogenized in 200 µl TriPure (Roche). Total RNA was DNAse treated, LiCl precipitated, reverse transcribed into cDNA, and quantified in a Light Cycler 480 System (Roche) using *ncam1* and *histone H4* primer sets listed in Table S5 and SYBR green detection. Quantitative PCR data were analyzed by $2^{-\Delta Ct}$ relative to *histone H4* (Schmittgen and Livak, 2008).

Immunohistochemistry on vibratome sections

Embryos were embedded in 4% low-melt agarose (Bio-Rad, 1613111) in 1× PBS under a dissection microscope in disposable molds (VWR, 15160-215). The embryos were sectioned coronally in cold 1× PBS using a Leica VT1200 vibratome (50 µm thickness, 1 mm amplitude, 0.5 mm/s speed). Free-floating vibratome sections were immunostained in mesh-bottomed baskets. Sections were permeabilized (0.5% Triton X-100) for 30 min then blocked (1% bovine serum albumin, 0.2% Triton X-100) in 1× PBS at room temperature. Incubation in primary antibody against either Myod (1:3) or 12/101 (1:10) (Developmental Studies Hybridoma Bank) was carried out in blocking buffer overnight at 4°C. Sections were washed three times for 15 min each wash in 0.2% Triton X-100 in 1× PBS then incubated in secondary antibody (donkey anti-mouse Alexa Fluor 647 1:200; Thermo Fisher Scientific) along with DAPI nuclear stain (1:2000). After washing again, sections were mounted on glass slides in antifade medium with 0.12 mm spacer (Thermo Fisher Scientific, S24735). Sections were imaged at 1.0 zoom on the Zeiss LSM880 confocal microscope at 20× magnification (Plan-Apochromat 1.3 numerical aperture) using a tiling stage and Zeiss Zen Black acquisition software.

Acknowledgements

We thank Dr Stefan Heller (Stanford University) for generous use of his lab's Leica VT1200 vibratome and the Stanford Otolaryngology Imaging Core (Lars Becker) for use of the Zeiss LSM700 confocal microscope, which were essential for Fig. 6 of this manuscript.

Competing interests

The authors declare no competing or financial interests.

Author contributions

Conceptualization: A.J., B.B.; Methodology: A.J., B.B.; Software: T.S.; Validation: A.J., W.T., B.B.; Formal analysis: A.J., W.T., T.S.; Investigation: A.J., W.T., T.S., B.B.; Resources: A.J., T.S., B.B.; Data curation: T.S.; Writing - original draft: A.J.; Writing - review & editing: A.J., B.B.; Visualization: A.J., W.T.; Supervision: A.J., B.B.; Project administration: A.J., B.B.; Funding acquisition: T.S., B.B.

Funding

This work was supported by grants from the National Science Foundation (IOS-0719576, IOS-1147236 to B.B.). A.J. is currently supported by the A.P. Giannini Foundation.

Data availability

RNA-seq data have been deposited in Gene Expression Omnibus under accession number GSE119124.

Supplementary information

Supplementary information available online at http://dev.biologists.org/lookup/doi/10.1242/dev.147769.supplemental

References

Aceto, N., Bardia, A., Miyamoto, D. T., Donaldson, M. C., Wittner, B. S., Spencer, J. A., Yu, M., Pely, A., Engstrom, A., Zhu, H. et al. (2014). Circulating tumor cell clusters are oligoclonal precursors of breast cancer metastasis. *Cell* **158**, 1110-1122.

Andreazzoli, M., Broccoli, V. and Dawid, I. B. (2001). Cloning and expression of noz1, a zebrafish zinc finger gene related to Drosophila nocA. *Mech. Dev.* **104**, 117-120.

Ang, H. L. and Duester, G. (1999). Stimulation of premature retinoic acid synthesis in Xenopus embryos following premature expression of aldehyde dehydrogenase ALDH1. *Eur. J. Biochem.* **260**, 227-234.

Arima, K., Shiotsugu, J., Niu, R., Khandpur, R., Martinez, M., Shin, Y., Koide, T., Cho, K. W., Kitayama, A., Ueno, N. et al. (2005). Global analysis of RAR-responsive genes in the Xenopus neurula using cDNA microarrays. *Dev. Dyn.* **232**, 414-431.

Bayha, E., Jørgensen, M. C., Serup, P. and Grapin-Botton, A. (2009). Retinoic acid signaling organizes endodermal organ specification along the entire antero-posterior axis. *PLoS One* **4**, e5845.

Beckmann, G. and Bork, P. (1993). An adhesive domain detected in functionally diverse receptors. *Trends Biochem. Sci.* **18**, 40-41.

Blumberg, B., Bolado, J., Jr, Derguini, F., Craig, A. G., Moreno, T. A., Chakravarti, D., Heyman, R. A., Buck, J. and Evans, R. M. (1996). Novel retinoic acid receptor ligands in Xenopus embryos. *Proc. Natl. Acad. Sci. USA* **93**, 4873-4878.

Blumberg, B., Bolado, J., Jr, Moreno, T. A., Kintner, C., Evans, R. M. and Papalopulu, N. (1997). An essential role for retinoid signaling in anteroposterior neural patterning. *Development* **124**, 373-379.

Bolce, M. E., Hemmati-Brivanlou, A., Kushner, P. D. and Harland, R. M. (1992). Ventral ectoderm of Xenopus forms neural tissue, including hindbrain, in response to activin. *Development* **115**, 681-688.

Cartry, J., Nichane, M., Ribes, V., Colas, A., Riou, J. F., Pieler, T., Dolle, P., Bellefroid, E. J. and Umbhauer, M. (2006). Retinoic acid signalling is required for specification of pronephric cell fate. *Dev. Biol.* **299**, 35-51.

Chal, J., Al Tanoury, Z., Hestin, M., Gobert, B., Aivio, S., Hick, A., Cherrier, T., Nesmith, A. P., Parker, K. K. and Pourquie, O. (2016). Generation of human muscle fibers and satellite-like cells from human pluripotent stem cells in vitro. *Nat. Protoc.* **11**, 1833-1850.

Chen, Y., Huang, L., Russo, A. F. and Solursh, M. (1992). Retinoic acid is enriched in Hensen's node and is developmentally regulated in the early chicken embryo. *Proc. Natl. Acad. Sci. USA* **89**, 10056-10059.

Cossu, G., Kelly, R., Di Donna, S., Vivarelli, E. and Buckingham, M. (1995). Myoblast differentiation during mammalian somitogenesis is dependent upon a community effect. *Proc. Natl. Acad. Sci. USA* **92**, 2254-2258.

Creech Kraft, J., Schuh, T., Juchau, M. R. and Kimelman, D. (1994). "Temporal distribution, localization and metabolism of all-trans-retinol, didehydroretinol and all-trans-retinal during Xenopus development." *Biochem J* **301**, 111-119.

Cunningham, T. J. and Duester, G. (2015). Mechanisms of retinoic acid signalling and its roles in organ and limb development. *Nat. Rev. Mol. Cell Biol.* **16**, 110-123.

De Domenico, E., Owens, N. D., Grant, I. M., Gomes-Faria, R. and Gilchrist, M. J. (2015). Molecular asymmetry in the 8-cell stage Xenopus tropicalis embryo described by single blastomere transcript sequencing. *Dev. Biol.* **408**, 252-268.

Diez del Corral, R., Olivera-Martinez, I., Goriely, A., Gale, E., Maden, M. and Storey, K. (2003). Opposing FGF and retinoid pathways control ventral neural pattern, neuronal differentiation, and segmentation during body axis extension. *Neuron* **40**, 65-79.

Durston, A. J., Timmermans, J. P., Hage, W. J., Hendriks, H. F., de Vries, N. J., Heideveld, M. and Nieuwkoop, P. D. (1989). Retinoic acid causes an anteroposterior transformation in the developing central nervous system. *Nature* **340**, 140-144.

Evans, R. M. and Mangelsdorf, D. J. (2014). Nuclear receptors, RXR, and the big bang. *Cell* **157**, 255-266.

Fletcher, R. B. and Harland, R. M. (2008). The role of FGF signaling in the establishment and maintenance of mesodermal gene expression in Xenopus. *Dev. Dyn.* **237**, 1243-1254.

Franco, P. (2002). *Rol del ácido retinoico durante la neurogénesis primaria de Xenopus laevis. PhD thesis*, Universidad de Buenos Aires.

Franco, H. L. and Yao, H. H. (2012). Sex and hedgehog: roles of genes in the hedgehog signaling pathway in mammalian sexual differentiation. *Chromosome Res.* **20**, 247-258.

Gurdon, J. B. (1988). A community effect in animal development. *Nature* **336**, 772-774.

Gurdon, J. B., Tiller, E., Roberts, J. and Kato, K. (1993). A community effect in muscle development. *Curr. Biol.* **3**, 1-11.

Harvey, R. P. (1992). MyoD protein expression in Xenopus embryos closely follows a mesoderm induction-dependent amplification of MyoD transcription and is synchronous across the future somite axis. *Mech. Dev.* **37**, 141-149.

Hasegawa, K. and Saga, Y. (2012). Retinoic acid signaling in Sertoli cells regulates organization of the blood-testis barrier through cyclical changes in gene expression. *Development* **139**, 4347-4355.

Haselman, J. T., Olmstead, A. W. and Degitz, S. J. (2015). Global gene expression during early differentiation of Xenopus (Silurana) tropicalis gonad tissues. *Gen. Comp. Endocrinol.* **214**, 103-113.
Holland, D. G., Burleigh, A., Git, A., Goldgraben, M. A., Perez-Mancera, P. A., Chin, S. F., Hurtado, A., Bruna, A., Ali, H. R., Greenwood, W. et al. (2011). ZNF703 is a common Luminal B breast cancer oncogene that differentially regulates luminal and basal progenitors in human mammary epithelium. *EMBO Mol. Med.* **3**, 167-180.
Hong, C. S. and Saint-Jeannet, J. P. (2017). Znf703, a novel target of Pax3 and Zic1, regulates hindbrain and neural crest development in Xenopus. *Genesis* **55**.
Hopwood, N. D., Pluck, A. and Gurdon, J. B. (1989). MyoD expression in the forming somites is an early response to mesoderm induction in Xenopus embryos. *EMBO J.* **8**, 3409-3417.
Hopwood, N. D., Pluck, A. and Gurdon, J. B. (1991). Xenopus Myf-5 marks early muscle cells and can activate muscle genes ectopically in early embryos. *Development* **111**, 551-560.
Hopwood, N. D., Pluck, A., Gurdon, J. B. and Dilworth, S. M. (1992). Expression of XMyoD protein in early Xenopus laevis embryos. *Development* **114**, 31-38.
Huang da, W., Sherman, B. T. and Lempicki, R. A. (2009a). Bioinformatics enrichment tools: paths toward the comprehensive functional analysis of large gene lists. *Nucleic Acids Res.* **37**, 1-13.
Huang da, W., Sherman, B. T. and Lempicki, R. A. (2009b). Systematic and integrative analysis of large gene lists using DAVID bioinformatics resources. *Nat. Protoc.* **4**, 44-57.
Janesick, A., Shiotsugu, J., Taketani, M. and Blumberg, B. (2012). RIPPLY3 is a retinoic acid-inducible repressor required for setting the borders of the pre-placodal ectoderm. *Development* **139**, 1213-1224.
Janesick, A., Abbey, R., Chung, C., Liu, S., Taketani, M. and Blumberg, B. (2013). ERF and ETV3L are retinoic acid-inducible repressors required for primary neurogenesis. *Development* **140**, 3095-3106.
Janesick, A., Nguyen, T. T., Aisaki, K., Igarashi, K., Kitajima, S., Chandraratna, R. A., Kanno, J. and Blumberg, B. (2014). Active repression by RARgamma signaling is required for vertebrate axial elongation. *Development* **141**, 2260-2270.
Janesick, A., Tang, W., Nguyen, T. T. L. and Blumberg, B. (2017). RARbeta2 is required for vertebrate somitogenesis. *Development* **144**, 1997-2008.
Karpinka, J. B., Fortriede, J. D., Burns, K. A., James-Zorn, C., Ponferrada, V. G., Lee, J., Karimi, K., Zorn, A. M. and Vize, P. D. (2015). Xenbase, the Xenopus model organism database; new virtualized system, data types and genomes. *Nucleic Acids Res.* **43**, D756-D763.
Kato, K. and Gurdon, J. B. (1993). Single-cell transplantation determines the time when Xenopus muscle precursor cells acquire a capacity for autonomous differentiation. *Proc. Natl. Acad. Sci. USA* **90**, 1310-1314.
Kayala, M. A. and Baldi, P. (2012). Cyber-T web server: differential analysis of high-throughput data. *Nucleic Acids Res.* **40**, W553-W559.
Koide, T., Downes, M., Chandraratna, R. A., Blumberg, B. and Umesono, K. (2001). Active repression of RAR signaling is required for head formation. *Genes Dev.* **15**, 2111-2121.
Loh, K. M., Chen, A., Koh, P. W., Deng, T. Z., Sinha, R., Tsai, J. M., Barkal, A. A., Shen, K. Y., Jain, R., Morganti, R. M. et al. (2016). Mapping the pairwise choices leading from pluripotency to human bone, heart, and other mesoderm cell types. *Cell* **166**, 451-467.
Maden, M. (2007). Retinoic acid in the development, regeneration and maintenance of the nervous system. *Nat. Rev. Neurosci.* **8**, 755-765.
Matsuda, Y., Uno, Y., Kondo, M., Gilchrist, M. J., Zorn, A. M., Rokhsar, D. S., Schmid, M. and Taira, M. (2015). A new nomenclature of xenopus laevis chromosomes based on the phylogenetic relationship to silurana/xenopus tropicalis. *Cytogenet Genome Res.* **145**, 187-191.
Moreno, T. A. and Kintner, C. (2004). Regulation of segmental patterning by retinoic acid signaling during Xenopus somitogenesis. *Dev. Cell* **6**, 205-218.
Nakaya, Y. and Sheng, G. (2008). Epithelial to mesenchymal transition during gastrulation: an embryological view. *Dev. Growth Differ.* **50**, 755-766.
Naylor, R. W., Skvarca, L. B., Thisse, C., Thisse, B., Hukriede, N. A. and Davidson, A. J. (2016). BMP and retinoic acid regulate anterior-posterior patterning of the non-axial mesoderm across the dorsal-ventral axis. *Nat. Commun.* **7**, 12197.
Niederreither, K., Vermot, J., Messaddeq, N., Schuhbaur, B., Chambon, P. and Dolle, P. (2001). Embryonic retinoic acid synthesis is essential for heart morphogenesis in the mouse. *Development* **128**, 1019-1031.
Pfeffer, P. L. and De Robertis, E. M. (1994). Regional specificity of RAR gamma isoforms in Xenopus development. *Mech. Dev.* **45**, 147-153.
Pijnappel, W. W., Hendriks, H. F., Folkers, G. E., van den Brink, C. E., Dekker, E. J., Edelenbosch, C., van der Saag, P. T. and Durston, A. J. (1993). The retinoid ligand 4-oxo-retinoic acid is a highly active modulator of positional specification. *Nature* **366**, 340-344.
Rhinn, M. and Dolle, P. (2012). Retinoic acid signalling during development. *Development* **139**, 843-858.
Rochette-Egly, C. and Germain, P. (2009). Dynamic and combinatorial control of gene expression by nuclear retinoic acid receptors (RARs). *Nucl. Recept. Signal.* **7**, e005.
Ruiz i Altaba, A. and Jessell, T. (1991). Retinoic acid modifies mesodermal patterning in early Xenopus embryos. *Genes Dev.* **5**, 175-187.
Schmittgen, T. D. and Livak, K. J. (2008). Analyzing real-time PCR data by the comparative CT method. *Nat. Protoc.* **3**, 1101-1108.
Schneider, V. A. and Mercola, M. (2001). Wnt antagonism initiates cardiogenesis in Xenopus laevis. *Genes Dev.* **15**, 304-315.
Session, A. M., Uno, Y., Kwon, T., Chapman, J. A., Toyoda, A., Takahashi, S., Fukui, A., Hikosaka, A., Suzuki, A., Kondo, M. et al. 2016). Genome evolution in the allotetraploid frog Xenopus laevis. *Nature* **538**, 336-343.
Seufert, D. W., Hegde, R. S., Nekkalapudi, S., Kelly, L. E. and El-Hodiri, H. M. (2005). Expression of a novel Ski-like gene in Xenopus development. *Gene Expr. Patterns* **6**, 22-28.
Shahi, P., Slorach, E. M., Wang, C. Y., Chou, J., Lu, A., Ruderisch, A. and Werb, Z. (2015). The transcriptional repressor ZNF503/Zeppo2 promotes mammary epithelial cell proliferation and enhances cell invasion. *J. Biol. Chem.* **290**, 3803-3813.
Shimono, K., Tung, W. E., Macolino, C., Chi, A. H., Didizian, J. H., Mundy, C., Chandraratna, R. A., Mishina, Y., Enomoto-Iwamoto, M., Pacifici, M. et al. (2011). Potent inhibition of heterotopic ossification by nuclear retinoic acid receptor-gamma agonists. *Nat. Med.* **17**, 454-460.
Shimshoni, J. A., Roberts, A. G., Scian, M., Topletz, A. R., Blankert, S. A., Halpert, J. R., Nelson, W. L. and Isoherranen, N. (2012). Stereoselective formation and metabolism of 4-hydroxy-retinoic Acid enantiomers by cytochrome p450 enzymes. *J. Biol. Chem.* **287**, 42223-42232.
Sive, H. L. and Cheng, P. F. (1991). Retinoic acid perturbs the expression of Xhox.lab genes and alters mesodermal determination in Xenopus laevis. *Genes Dev.* **5**, 1321-1332.
Sive, H. L., Draper, B. W., Harland, R. M. and Weintraub, H. (1990). Identification of a retinoic acid-sensitive period during primary axis formation in Xenopus laevis. *Genes Dev.* **4**, 932-942.
Slorach, E. M., Chou, J. and Werb, Z. (2011). Zeppo1 is a novel metastasis promoter that represses E-cadherin expression and regulates p120-catenin isoform expression and localization. *Genes Dev.* **25**, 471-484.
Sokol, S., Wong, G. G. and Melton, D. A. (1990). A mouse macrophage factor induces head structures and organizes a body axis in Xenopus. *Science* **249**, 561-564.
Standley, H. J., Zorn, A. M. and Gurdon, J. B. (2001). eFGF and its mode of action in the community effect during Xenopus myogenesis. *Development* **128**, 1347-1357.
Symes, K., Yaqoob, M. and Smith, J. C. (1988). Mesoderm induction in Xenopus laevis: responding cells must be in contact for mesoderm formation but suppression of epidermal differentiation can occur in single cells. *Development* **104**, 609-618.
Topletz, A. R., Tripathy, S., Foti, R. S., Shimshoni, J. A., Nelson, W. L. and Isoherranen, N. (2015). Induction of CYP26A1 by metabolites of retinoic acid: evidence that CYP26A1 is an important enzyme in the elimination of active retinoids. *Mol. Pharmacol.* **87**, 430-441.
Torres, J., Prieto, J., Durupt, F. C., Broad, S. and Watt, F. M. (2012). Efficient differentiation of embryonic stem cells into mesodermal precursors by BMP, retinoic acid and Notch signalling. *PLoS ONE* **7**, e36405.
Trapnell, C., Roberts, A., Goff, L., Pertea, G., Kim, D., Kelley, D. R., Pimentel, H., Salzberg, S. L., Rinn, J. L. and Pachter, L. (2012). Differential gene and transcript expression analysis of RNA-seq experiments with TopHat and Cufflinks. *Nat. Protoc.* **7**, 562-578.
Tsang, K. Y., Sinha, S., Liu, X., Bhat, S. and Chandraratna, R. A. (2003). Disubstituted chalcone oximes having RARy retinoid receptor antagonist activity. https://patents.google.com/patent/US20050165095

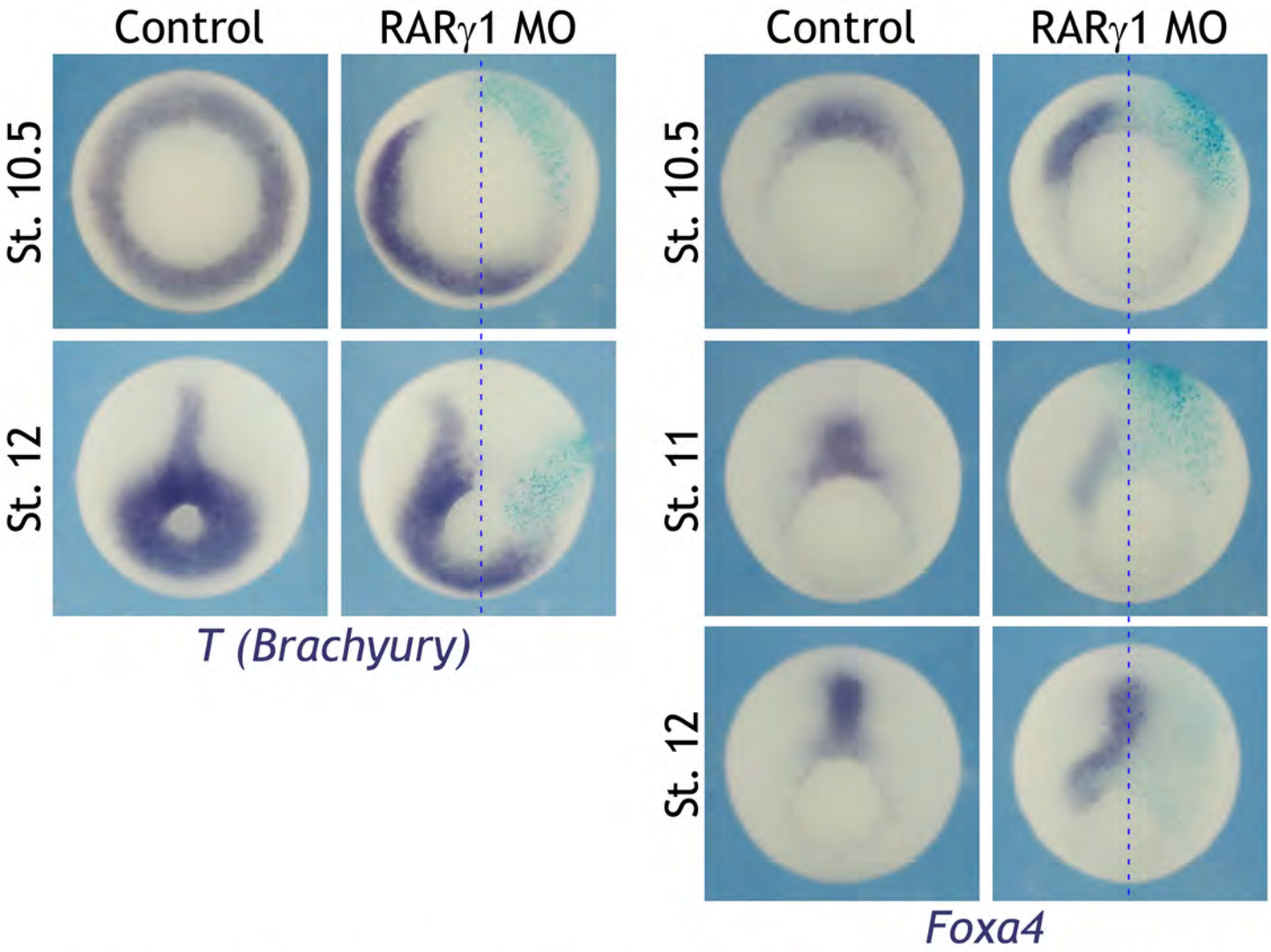

Supplemental Figure S1. RARγ1 is required for the expression of mesoderm markers. Embryos were microinjected unilaterally at the 2-cell or 4-cell stage with 10 ng *Rarγ1*.L/S MO (see Fig S3). Injected side is to the right of the dotted line, and is indicated by the turquoise *β-gal* lineage tracer. *Rarγ1* MO results in the loss of *T (Brachyury)* and *Foxa4*.

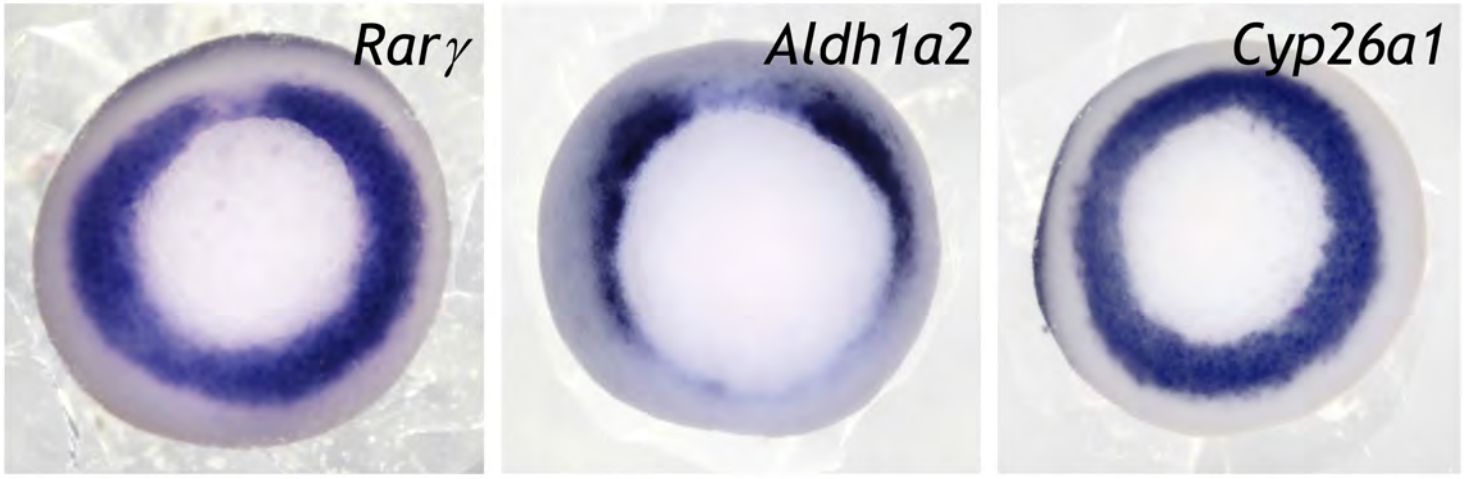

Supplemental Figure S2. Whole mount in situ hybridization showing the expression of *Rarγ*, *Aldh1a2*, and *Cyp26a1* at stage 10.5/11, vegetal view, dorsal lip at the top.

>X. laevis Chromosome 2.S

tcttccacctaaggtttataatggatttatcgctgaataactaaggaagacattg
gtacccaaggaagattccaagacaactactggctagcactaagtaagagactgag
ctagaacaaggca(ATG)GCAAACAGCAGCAAGGAGCGCCTCTGTG

>X. laevis Chromosome 2.L

tcttctacctaaggtgtatcatggatttattgctgaataactaaggaagactttg
gtacccaaagaagattccagga-aactactggctagaactcagtgagagactgag
ggagaacaaggca(ATG)GCAAACAGCAGCAAGGAGCGCCTCTGTG

RARγ1 MO #1 RARγ1 MO #2

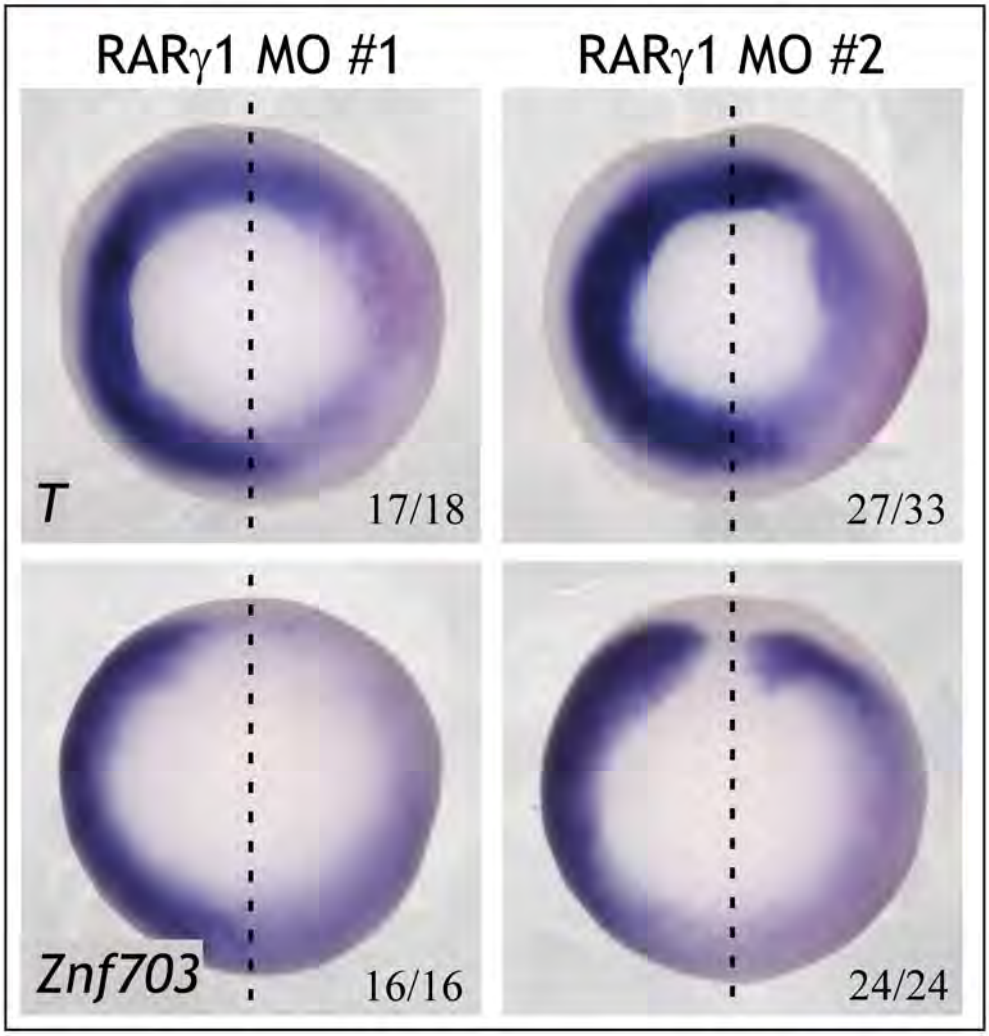

Supplemental Figure S3. Specificity of RARγ1 MO phenotype. Two different morpholinos were designed to target *Xenopus laevis Rarγ1*. **(Top)** Mapping of MOs to the .S and .L subgenomes (Session, 2016). MO#1 matches nearly perfectly to both .S and .L, whereas MO #2 matches only .S, and will not likely to bind .L. **(Bottom)** Embryos were microinjected unilaterally at the 2-cell or 4-cell stage with 6.6 ng of either *Rarγ1.L/S* MO (#1) or *Rarγ1.S* (#2). Injected side is to the right of the dotted line, and is indicated by the magenta *β-gal* lineage tracer. RARγ1 MO #1 and MO#2 give the same knockdown phenotype on *T* and *Znf703*. Fractions represent the portion of embryos displaying the phenotype.

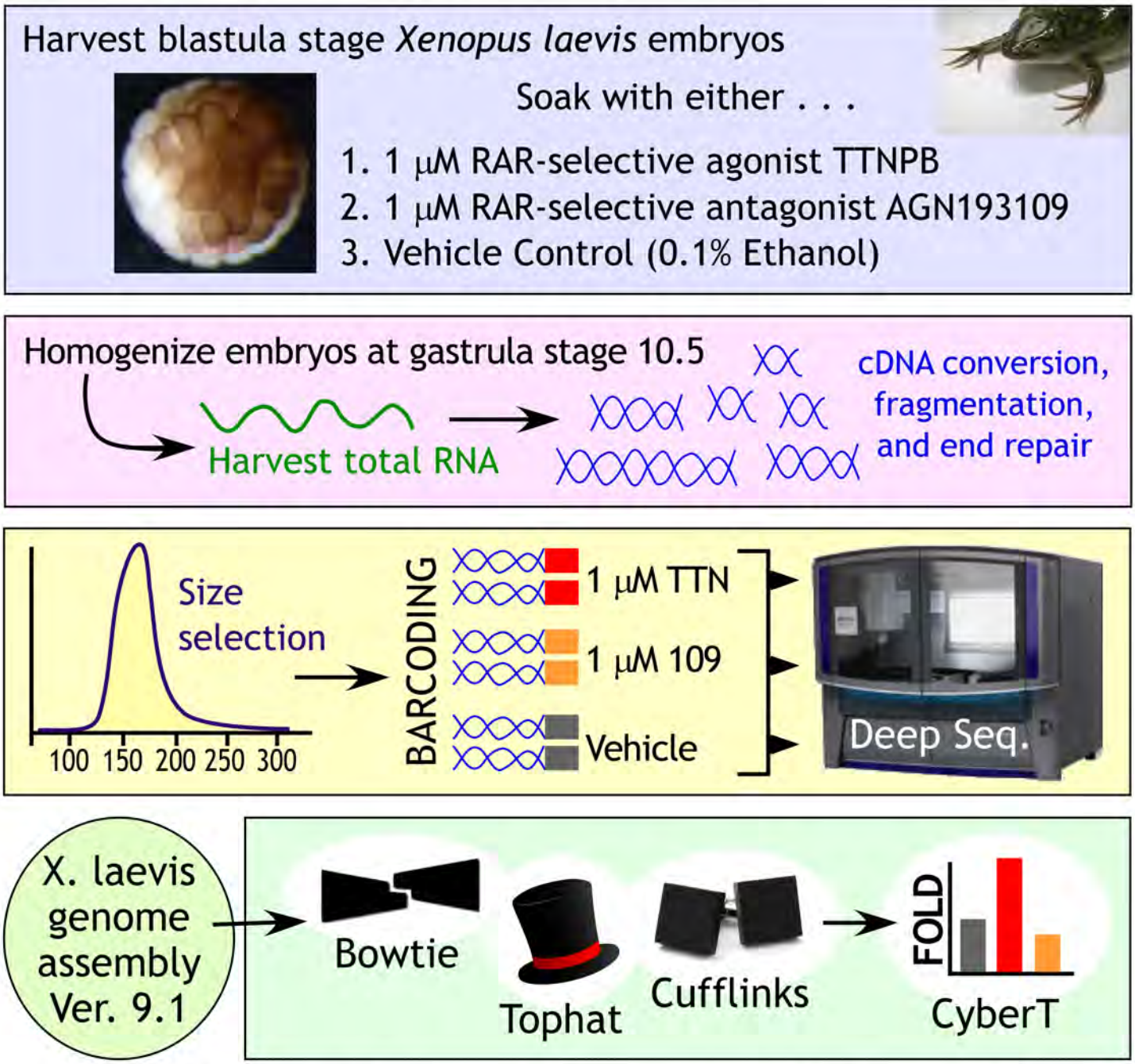

Supplemental Figure S4. Schematic of the experimental design and RNA-Seq pipeline. Total RNA was isolated from gastrula (stage 10.5) embryos that had been treated at the early blastula (stage 6) with control vehicle (0.1% ethanol), RAR-selective agonist TTNPB (TTN), or RAR-selective antagonist AGN193109 (109). After cDNA synthesis, multiplexed sequencing reactions were run (Aceto et al., 2014). Reads were mapped to *X. laevis* genome v9.1 (Session et al., 2016) using Bowtie, TopHat and Cufflinks algorithms.

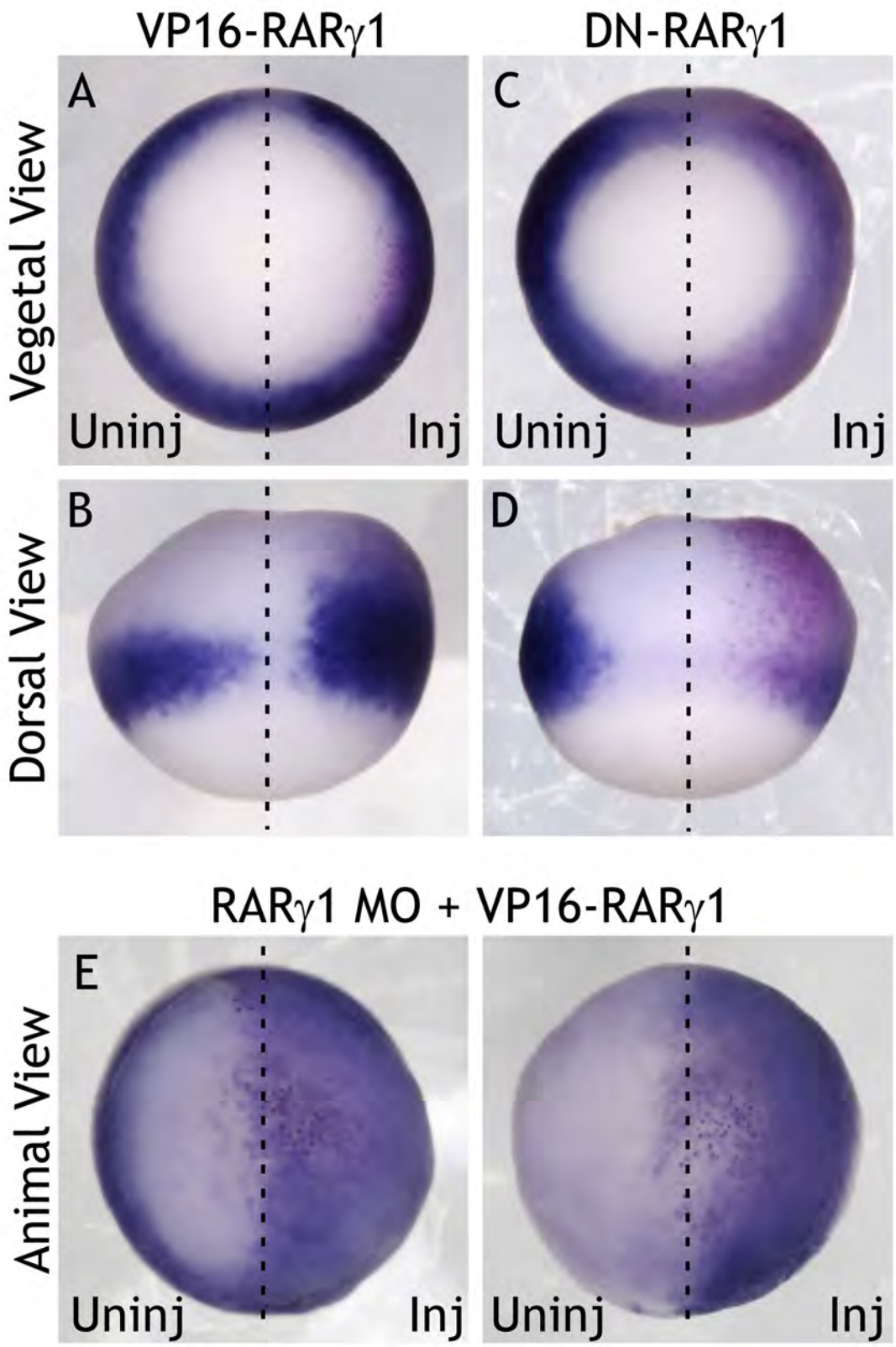

Supplemental Figure S5. VP16-*Rarγ1* mRNA expands *Znf703* while DN-*Rarγ1* mRNA diminishes *Znf703*. (A-E) Embryos were injected unilaterally at 2- or 4-cell stage. Injected side is to the right of the dotted line, and is indicated by magenta *ß-gal* lineage tracer. **(A, B, E)** 0.2 ng VP16-*Rarγ1* mRNA expands *Znf703* dorsally and animally. **(C, D)** 2 ng DN-*Rarγ1* mRNA diminishes *Znf703*. Embryos are shown at stage 10.5/11 in vegetal **(A, C)**, dorsal **(B, D)** or animal **(E)** view.

Supplemental Table S1 (1 µM TTNPB) – see Excel sheet
Supplemental Table S2 (1 µM AGN193109) – see Excel sheet

Click here to Download Tables S1 & S2

Supplemental Table S3 (Morpholinos)

MO	Sequence (5'→3')
Rarα2.L	ATC CAA AGG AAG GTG AGT GTG TGT G
Rarα2.S	CTG AAA TCC AAA CTG ACC ATA GAG T
Rarγ1.L/S	GCT GTT TGC CAT TGC CTT GTT CTA
Rarγ1.S	CTA GCC AGT AGT TGT CTT GGA ATC T

Supplemental Table S4 (Probe Design)

Probes with T7 Adapters

Primer	Sequence (5'→3')
Aldh1a2_Probe_For	ACCCTTGAATCTCTAAACAGTGGC
Aldh1a2_Probe_Rev	taatacgactcactatagggAATCTCTTCTCTGGCAATCCGCA
Cyp26a1_Probe_For	GCAGGTTCCTCCAAGTGAAGC
Cyp26a1_Probe_Rev	taatacgactcactatagggCCGCAGAGTCTCCTTAATGACAC
T_Probe_For	GAACGTACAGTACCGGGTGGA
T_Probe_Rev	taatacgactcactatagggTGGTGTGATGGCACTGTTACTC
Gdf3_Probe_For	CTCAGTCTTTCCGTCTCCTTCAC
Gdf3_Probe_Rev	taatacgactcactatagggCAACCACACTCATCCACTACCA
Wnt8_Probe_For	CAACTCTTCTGATCTTCTGCCCA
Wnt8_Probe_Rev	taatacgactcactatagggGTGATTGCCAATATCCCGAAACTC
Skida1_Probe_For	CTGGAGTCGGGCTATGAAGTGG
Skida1_Probe_Rev	taatacgactcactatagggTCCTCCTGTGCCTGTAAGTGG
Kielin_Probe_For	ATTCTGTTGCCACTTCTCTTCTCC
Kielin_Probe_Rev	taatacgactcactatagggATCTCTTCATCCTCCATTTGACGC
Kremen2_Probe_For	TGTTGGTGGAGATGCTGTGG
Kremen2_Probe_Rev	taatacgactcactatagggTCTGGAATCTGGAAGATGTGGA
Nkx6.2_Probe_For	GCCGAGATGAAGACCACTCTG
Nkx6.2_Probe_Rev	taatacgactcactatagggCTCCTCGTTGTCTGAACTCTCC
Mamdc2_Probe_For	ACAGGAAGGGATGTTCTTTGATGC
Mamdc2_Probe_Rev	taatacgactcactatagggTGGCTTTCTGTCCAAACACCA
Znf703_Probe_For	AGCTGAATTCTGTGACCTCCAG
Znf703_Probe_Rev	taatacgactcactatagggCATAAAGCCGTAGGTGTACAAGG
Znf503_Probe_For	CCACTGGGTTCTGGAAGTCG
Znf503_Probe_Rev	taatacgactcactatagggTTTATAGGGTGACACAGGTGC
Dhh_Probe_For	TGCCTAATGTGCCAGAGAAGACTC
Dhh_Probe_Rev	taatacgactcactatagggACAGATGATTGGGTGTAACAAGGA
Btg2_Probe_For	CTCCCGAAAGTCAGCAAGACAC
Btg2_Probe_Rev	taatacgactcactatagggAGACACAAATTGAACCGTCCTCTC
Hapln3_Probe_For	CTTGCCGAATTTGCTGTGATTCTC
Hapln3_Probe_Rev	taatacgactcactatagggGTTCTCCGTAGCTTCTAACACCA
Fstl1_Probe_For	GAGCCCAAGAGCAAGTCTAAGG
Fstl1_Probe_Rev	taatacgactcactatagggCAGATGGTTGGAAGTCGGGA

Supplemental Table S5 (QPCR)

Primer	Sequence (5'→3')
F (*Histone H4*):	GAT AAC ATC CAG GGC ATC AC
R (*Histone H4*):	TAA CCT CCG AAT CCG TAC AG